CBPF - CENTRO BRASILEIRO DE PESQUISAS FÍSICAS

Rio de Janeiro

Notas de Física

Thermostatistics of a damped bi-modal particle

João R. Medeiros and Sílvio M. Duarte Queirós

GOVERNO FEDERAL

BRASIL

PÁTRIA EDUCADORA

Thermostatistics of a damped bi-modal particle

João R. Medeiros and Sílvio M. Duarte Queirós

Centro Brasileiro de Pesquisas Físicas and

National Institute of Science and Technology for Complex Systems

Rua Dr Xavier Sigaud, 150, 22290-180 Rio de Janeiro — RJ, Brazil

Abstract

We study the thermostatistics of a damped bi-modal particle, *i.e.*, a particle of mass m subject to a work reservoir that is analytically represented by the telegraph noise. Because of the coloured nature of the noise, this system does not fit the Lévy-Itô class of stochastic processes making of it an instance of a non-equilibrium system in contact with an external reservoir. We obtain the statistics for the position and velocity, namely in the steady state, as well as the (time dependent) statistics of the energy fluxes in the system considering no constraints on the noise features. With that results we are able to give an account of the statistical features of the large deviations of the injected and dissipated power that can change from sub-Gaussianity to super-Gaussianity depending on the colour of the noise. By properly defining an effective temperature for this system, $\mathcal{T}$, we are capable of obtaining an equivalent entropy production/exchange rate equal to the ratio between the dissipation of the medium, γ, and the mass the particle, a relation that concurs with the case of a standard thermal reservoir at temperature, $T = \mathcal{T}$.

I. INTRODUCTION

The problem of Brownian diffusion as studied by Smoluchowski and Einstein or other more generic cases that fit the Kramers Equation allow describing the probabilistic behaviour of a particle of mass m — which we dub *focal particle* — in a medium wherewith it continuously exchanges heat. It is this endless energy exchange related to an unceasing production of entropy that makes of this kind of systems a paradigmatic case of non-equilibrium statistical mechanics. From these models, it is possible to establish relations between dynamical features of the focal particle — *e.g.*, typical square velocity and diffusivity — with physical properties of the medium like its dissipation constant, temperature and other physical constraints the particle is subject to, like the form of a confining or interacting potential for example [1].

From the perspective of a description in the space of physical observables (position and velocity), problems related to Brownian motion are based on the Langevin equation, which assumes that in a infinitesimal interval of time the focal particle suffers a large number of collisions with the particles of the medium. Furthermore, those collisions relax instantaneously and act upon the particle independently one another. Under this set of assumptions, the outcome is a Gaussian stochastic force.

Nowadays, it is well known that non-equilibrium situations corresponding to the Langevin equation with standard Gaussian terms (either white or coloured) represent a small stake of the problems that surround us [2–7]. For instance, we just need to consider a little dense medium for which the impacts of the focal particle occur at relevant rates, *e.g.*, the order of the (inverse of the) relaxation scale of the system. Other cases include molecular motors [5, 8, 9] or colloidal systems [10]. In not being described by Gaussian noise, the cumulants of order greater or equal than three do not vanish, which means that a probabilistic treatment of the problem based on solving an associated Fokker-Planck (or Kramers) equation is, at best, an approximation.

These non-Gaussian noise features pose interesting questions regarding its impact on the thermostatistical behaviour of the system. Explicitly, according to the Lévy-Itô theorem on the decomposition of the measure, any white noise can be written as the superposition of continuous measure Brownian motion (Gaussian noise) and singular measure Poissonian motion (shot-noise) [11]. Recently, it was proved that shot-noise systems can

have radically different transport properties, namely when the system has got non-linear elements [12–15].

Nevertheless, there are still many situations that do not fit the superposition of white noises; that is the case of the telegraph noise (also known as dichotomous or 2-state Brownian noise) which can assume two values that randomly alternate between them at given specific rates [16–18] and whose treatment in probability space is not compatible with the Fokker-Planck Equation. Besides the evident theoretical interest that a different type of noise prompts, the telegraph noise is appropriate to a quantitative description of nanomechanical problems like intracellular bidirectional transport on cytoskeletal filaments mediated by two sets of molecular motors — namely the Kinesin-1 and cytoplasmic Dinein — that pull the load in opposite directions similar to a random tug-of-war [21] or the kinetics of protein markers in capillary media, *e.g.*, the dynamics of calcium ions in blood plasma [22] as well as manometric ratchets [23]. Additionally, the telegraph noise fits the description of transport properties in amorphous materials [24], chromatography [25], quantum effects [26–28] among other systems and phenomena.

Owing to its analytical complexity, the problem of dichotomous noise has been treated considering simplifications, namely overdamping and equal transition rates between states as well as symmetrical values for the states [29–31]. However, even for such conditions the achievement a utterly exact and closed solution to the probability density functions is strict. That said, the main focus of this problem has been the computation of the probability currents, which are a proxy for the average velocities, the moments of the velocity and correlations, always considering an overdamped limit with symmetric noise.

The present paper aims to treat the generic model of a particle subject to a telegraph noise without considering any of the restrictions aforementioned. Besides the statistical characterisation of position and velocity, we introduce a thermostatistical survey of the system, namely on the fluxes of heat and work that can be related to large deviation functions of power and to entropy production and exchange by the system. The intermingle of time independent and time dependent results permits to establish a proper definition of (effective) temperature of this actually athermal system.

II.   THE MODEL

The evolution of the position, x, and velocity, v, of our focal particle with mass, m, is defined by the set of equations,

$$\begin{cases} m\dfrac{dv(t)}{dt} &= -\gamma\, v\,(t) - k\; x\,(t) - \zeta_t \\[2ex] v\,(t) &= \qquad\quad \dfrac{dx(t)}{dt} \end{cases}, \tag{1}$$

representing the fact that it is constrained by a harmonic potential ($k\, x^2/2$) and subject to dissipation (with constant γ) and a stochastic force, ζ, describing the interaction between the particle and the (work) reservoir. From a physical point of view, the potential can mimic the action of an optical tweezer that has a behaviour very close to harmonicity [19].

Analytically, the telegraph noise corresponds to a stochastic process, $\{\zeta_t\}$ that assumes two values, $\zeta = \{a, b\}$. In time, one either has $\zeta = a$ or $\zeta = b$ according to the transition rates,

- μ, from b to a;

- $\bar{\mu} = \rho\,\mu$, from a to b.

These conditions allow writing a Master Equation (see A) that yields a stationary distribution,

$$f_{\text{ss}}\,(\zeta) = p\,\delta_{a,\zeta} + \bar{p}\,\delta_{b,\zeta}, \tag{2}$$

with,

$$p \equiv \frac{\mu}{\mu + \bar{\mu}} = \frac{\mu}{\mu\,(1 + \rho)} = \frac{\mu}{\mu\,\hat{\rho}} = \hat{\rho}^{-1}, \qquad \bar{p} \equiv 1 - p = \frac{\hat{\rho} - 1}{\hat{\rho}}. \tag{3}$$

At this point, we address the reader to A for further details on the statistics of the noise. In the stationary state the correlation function,

$$\langle\langle \zeta\,(t_1)\; \zeta\,(t_2)\rangle\rangle \equiv \langle \zeta\,(t_1)\; \zeta\,(t_2)\rangle - \langle \zeta\,(t_1)\rangle\, \langle \zeta\,(t_2)\rangle, \tag{4}$$

reads,

$$\langle\langle \zeta\,(t_1)\; \zeta\,(t_2)\rangle\rangle = \Delta^2\, P\, e^{-\alpha\,|t_1 - t_2|}, \tag{5}$$

where,

$$\Delta \equiv a - b, \qquad \alpha \equiv \mu \left(1 + \rho\right) = \mu \, \hat{\rho} \qquad P \equiv p \, \bar{p}. \tag{6}$$

From Eq. (5), we verify that the telegraph noise is not white; hence, the Lévy-Itô theorem on the composition of the measure does not apply and the problem of a bi-modal particle fits into a different category. Moreover, since the fluctuations induced by ζ in the system are coloured and the dissipation only depends on the value of the velocity at time t (and not its past values), the fluctuations and the dissipation do not have the same origin and thus the reservoir is is classified as external, *i.e.*, it does not abide by the fluctuation-dissipation relation [32]. As a matter of fact, taking into consideration the two state properties of the noise we can deem a dichotomous athermal reservoir as a work reservoir since it performs work by pulling and pushing the focal particle for random periods of time.

Looking at Eq. (1), we identify the following time scales: a time scale imposed by the medium,

$$\tau_r \equiv \frac{m}{\gamma}, \tag{7}$$

that is associated with the existence of dissipation leading to a stationary solution in the velocity and a time scale related to the confining potential,

$$\tau_s \equiv \sqrt{\frac{m}{k}}, \tag{8}$$

that will be associated with oscillatory terms. In addition, there are time scales relate to the noise; a scale defined by the colour of the noise,

$$\tau \equiv \alpha^{-1}, \tag{9}$$

and the typical time the noise has a value $\zeta = a\left(b\right)$,

$$\tau_a \equiv \bar{\mu}^{-1}, \qquad \tau_b \equiv \mu^{-1}.$$

The formulation in the space of observables provided by Eq. (1) bridges with a description of the process in the space of the probabilities. Imposing, $f\left(x, v, t_0 \mid x_0, v_0, t_0\right) = \delta\left(x - x_0\right) \delta\left(v - v_0\right)$ as the initial condition, the evolution of the probability density func-

tion is given by,

$$
\begin{cases}
\frac{\partial}{\partial t} f'(x, v, a, t) = \left[-\frac{\partial}{\partial x} v + \frac{\partial}{\partial v} \frac{\gamma v + k x - a}{m} \right] f'(x, v, a, t) + \mu f'(x, v, b, t) - \bar{\mu} f'(x, v, a, t) \\
\\
\frac{\partial}{\partial t} f'(x, v, b, t) = \left[-\frac{\partial}{\partial x} v + \frac{\partial}{\partial v} \frac{\gamma v + k x - b}{m} \right] f'(x, v, b, t) + \bar{\mu} f'(x, v, a, t) - \mu f'(x, v, b, t)
\end{cases},
$$

(10)

with,

$$
f(x, v, t) = \sum_{\zeta} f'(x, v, \zeta, t). \tag{11}
$$

The visual inspection of Eq. (10) give us an indication about the intricate character of the solution to this problem and explains the simplifications introduced in previous works. For this reason we scrapped solving Eqs. (10) and (11) and opted to directly treat Eq. (1) resorting to Laplace-Fourier transforms.

A. Method of solution

Let us define the Laplace-Fourier transform as,

$$
\widetilde{\mathcal{O}}(i q + \varepsilon) \equiv \lim_{\varepsilon \to 0} \int \mathcal{O}(t) \, e^{-(i q + \varepsilon) t} \, dt. \tag{12}
$$

After Fourier-Laplace transforming, Eq. (1) becomes,

$$
\begin{cases}
m (i q + \varepsilon) \tilde{v}(i q + \varepsilon) = -\gamma \tilde{v}(i q + \varepsilon) - k \tilde{x}(i q + \varepsilon) + \tilde{\zeta}(i q + \varepsilon) \\
\\
\tilde{v}(t) = (i q + \varepsilon) \tilde{x}(i q + \varepsilon)
\end{cases}. \tag{13}
$$

Plugging the second line in the first one, we eliminate the velocity and we have for the position in reciprocal space,

$$
\tilde{x}(i q + \varepsilon) = \frac{\tilde{\zeta}(i q + \varepsilon)}{R(i q + \varepsilon)}. \tag{14}
$$

The function $R(s)$ is,

$$
R(s) = m (s - \kappa_+)(s - \kappa_-), \tag{15}
$$

with zeros located at,

$$
\kappa_\pm = -\frac{\theta}{2} \pm i \Omega
$$

(16)

$$
= -\frac{\theta}{2} \pm i \sqrt{4 \omega^2 - \theta^2},
$$

where,

$$\theta = \tau_r^{-1} = \frac{\gamma}{m}, \qquad \omega^2 = \tau_o^{-2} = \frac{k}{m}. \tag{17}$$

Because the thermostatistical behaviour of the system is ruled by the position, velocity or (stochastic) force, we consider a generic quantity, $\mathcal{O}(t)$, that in reciprocal space is recast as,

$$\widetilde{\mathcal{O}}(\mathrm{i}\,q_1 + \varepsilon) = h(\mathrm{i}\,q_1 + \varepsilon)\,\tilde{x}(\mathrm{i}\,q_1 + \varepsilon). \tag{18}$$

Accordingly, we have: for the velocity $h_v(s) = s$, for the position $h_x(s) = 1$ and for the noise $h_\zeta(s) = R(s)$.

As we already mentioned, this system reaches a stationary state and under this circumstance the ergodic property,

$$\langle \mathcal{O} \rangle = \overline{\mathcal{O}} \equiv \lim_{\Xi \to \infty} \frac{1}{\Xi} \int \mathcal{O}(t)\ dt. \tag{19}$$

relating averages over samples, $\langle \mathcal{O} \rangle$, and averages over time, $\overline{\mathcal{O}}$, holds. We can connect the computation with the Laplace-Fourier transform by means of the final value theorem [20],

$$\overline{\mathcal{O}} = \lim_{\Xi \to \infty} \frac{1}{\Xi} \int \mathcal{O}(t)\ dt = \lim_{z \to 0} z \int \mathrm{e}^{-z\,t}\,\mathcal{O}(t)\ dt. \tag{20}$$

Using Eq. (12) in Eq. (20) as well as the equality between time and sample averaging in the stationary state we get,

$$\langle \mathcal{O} \rangle = \lim_{z \to 0,\,\varepsilon \to 0} z \int \frac{dq}{2\pi} \int dt\,\mathrm{e}^{-z\,t + (\mathrm{i}\,q + \varepsilon)\,t}\,\langle \mathcal{O}(\mathrm{i}\,q + \varepsilon) \rangle \tag{21}$$

$$\langle \mathcal{O} \rangle = \lim_{z \to 0,\,\varepsilon \to 0} \int \frac{dq}{2\pi} \frac{z}{z - (\mathrm{i}\,q + \varepsilon)}\,\langle \mathcal{O}(\mathrm{i}\,q + \varepsilon) \rangle.$$

If we are interested in obtaining time dependent statistics, we can continue using the Laplace-Fourier representation but without applying the final value theorem,

$$\langle \mathcal{O}(t) \rangle = \lim_{\varepsilon \to 0} \int \frac{dq}{2\pi}\,\mathrm{e}^{(\mathrm{i}\,q + \varepsilon)\,t}\,\langle \mathcal{O}(\mathrm{i}\,q + \varepsilon) \rangle. \tag{22}$$

For the n-th order moment, the respective equation is straightforward from Eqs. (18) and (21),

$$\langle \mathcal{O}^n \rangle = \lim_{z \to 0,\,\varepsilon \to 0} \int \frac{z}{z - \sum_{l=1}^{n} (\mathrm{i}\,q_l + \varepsilon)} \frac{h(\mathrm{i}\,q_1 + \varepsilon) \ldots h(\mathrm{i}\,q_n + \varepsilon)}{R(\mathrm{i}\,q_1 + \varepsilon) \ldots R(\mathrm{i}\,q_n + \varepsilon)} \tag{23}$$

$$\times \left\langle \tilde{\zeta}(\mathrm{i}\,q_1 + \varepsilon) \ldots \tilde{\zeta}(\mathrm{i}\,q_n + \varepsilon) \right\rangle \frac{dq_1}{2\pi} \ldots \frac{dq_n}{2\pi}.$$

The multiple integration in $q_1, \ldots, q_n$ eliminates all the modes related to the transient. Analytically, this means that only combinations of poles that lead to a final expression proportional to z/z yield an *a priori* non-vanishing solution. Only terms proportional to $\left[\sum_{l=1}^{\ell} \left(\mathrm{i}\, q_l + \varepsilon \right) \right]^{-1}$ are in agreement with that condition. As clear from $R\left(q\right)$, those terms arise from the moments of the noise $\left\langle \tilde{\zeta} \left(\mathrm{i}\, q_1 + \varepsilon \right) \ldots \tilde{\zeta} \left(\mathrm{i}\, q_n + \varepsilon \right) \right\rangle$. In Fig. 1, we introduce the typical structure of the poles related to Eqs. (21) and (23). When the reservoir is
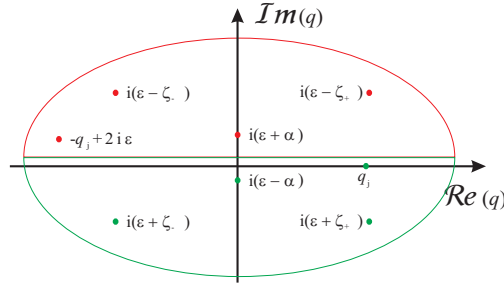

FIG. 1.   Location of the poles of Eq. (23) in the complex plane. The poles in the lower-arch will only be relevant in time dependent calculations.

Gaussian, the computation of $\left\langle \tilde{\zeta} \left(\mathrm{i}\, q_1 + \varepsilon \right) \ldots \tilde{\zeta} \left(\mathrm{i}\, q_n + \varepsilon \right) \right\rangle$ is quite simplified because it is possible to apply the Isserlis-Wick theorem. However, the distribution of the dichotomous reservoir is bimodal; that theorem does not apply and $\left\langle \tilde{\zeta} \left(\mathrm{i}\, q_1 + \varepsilon \right) \ldots \tilde{\zeta} \left(\mathrm{i}\, q_n + \varepsilon \right) \right\rangle$ has to be computed without further simplifications besides time ordering. This generally ends up giving quite long expressions. Nevertheless, we can grasp that,

$$\left\langle \tilde{\zeta} \left(\mathrm{i}\, q_1 + \varepsilon \right) \ldots \tilde{\zeta} \left(\mathrm{i}\, q_n + \varepsilon \right) \right\rangle \propto \prod_{i=1}^{n} \left[\sum_{j=1}^{i} \left(\mathrm{i}\, q_j + \varepsilon \right) \right]^{-1} \prod_{l=1}^{n-1} \left[\sum_{j=1}^{l} \left(\mathrm{i}\, q_j + \varepsilon \right) + \alpha \right]^{-1}. \quad (24)$$

where the first product contains the terms that give rise to non-vanishing calculations of the long term moments. We must emphasise that this method can be employed to both long term and time dependent statistics as we will demonstrate for the heat fluxes. In that case, the poles of the first product lead to the emergence of the explicit time dependencies whereas the second product will lead to damped oscillatory terms.

III.   RESULTS FOR THE LONG-TERM MOMENTS OF THE VELOCITY AND POSITION

In this section, we intensively use Eq. (23) for $\mathcal{O} = v$ and $\mathcal{O} = x$ that imply $h\left(i\,q_j + \varepsilon\right) = \left(i\,q_j + \varepsilon\right)$ and $h\left(i\,q_j + \varepsilon\right) = 1$, respectively.

For the averages, $n = 1$, we have,

$$\langle v \rangle = 0, \tag{25}$$

and,

$$\langle x \rangle = \frac{a\,p + b\,\bar{p}}{k}. \tag{26}$$

The value $\langle v \rangle = 0$ is a necessary condition for the existence of a global stationary state, for $\langle v \rangle \neq 0$ would lead to a time dependent average value of the position. Equation (25) is independent of the values assumed for the states of the noise $\{a, b\}$ and its weights $\{p, \bar{p}\}$ as well. In other words, during the transient, the system displaces from $x\,(t = 0) = 0$ to fluctuate around the average position Eq. (26), which is not a minimum of the potential. As we shall see this means that there is an energy cost to maintain that steady state.

For the variances, $\left\langle\left\langle \mathcal{O}^2 \right\rangle\right\rangle = \left\langle \mathcal{O}^2 \right\rangle - \left\langle \mathcal{O} \right\rangle^2$, we have,

$$\left\langle\left\langle v^2 \right\rangle\right\rangle = \left\langle v^2 \right\rangle = \frac{\Delta^2\,P\,\alpha}{\gamma\,\hat{k}}, \tag{27}$$

where,

$$\hat{k} \equiv k + \alpha\,(\gamma + m\,\alpha). \tag{28}$$

The second cumulant of the position reads,

$$\left\langle\left\langle x^2 \right\rangle\right\rangle = \frac{\Delta^2\,P\,\hat{\gamma}}{\gamma k\,\hat{k}}, \tag{29}$$

with,

$$\hat{\gamma} \equiv \gamma + m\,\alpha. \tag{30}$$

The value of $\langle v^2 \rangle$ plays a relevant role in non-equilibrium problems since it is related to the canonical (local) temperature of the system. Because the telegraph noise is the

stochastic process characterising our dichotomous reservoir, we christen the canonical temperature of a bimodal particle the *Marconi temperature* which reads,

$$\langle K \rangle \equiv \frac{1}{2} m \left\langle v^2 \right\rangle = \frac{1}{2} \mathcal{T},$$

$$\mathcal{T} = \frac{\Delta^2 P \left(\hat{\gamma} - \gamma \right)}{\gamma \, \hat{k}}. \tag{31}$$

Using $\mathcal{T}$, we recast the form of $\left\langle\!\left\langle x^2 \right\rangle\!\right\rangle$ into,

$$\left\langle\!\left\langle x^2 \right\rangle\!\right\rangle = \frac{\hat{\gamma}}{k \, (\hat{\gamma} - \gamma)} \mathcal{T}, \tag{32}$$

that is different from the value obtained for a particle subject to a harmonic potential and in contact with a thermal reservoir with temperature $T = \mathcal{T}$, $\left\langle\!\left\langle x^2 \right\rangle\!\right\rangle = \mathcal{T} k^{-1}$, which is its white-noise asymptotic limit.[1] The convergence of $\left\langle\!\left\langle v^2 \right\rangle\!\right\rangle$ and $\left\langle\!\left\langle x^2 \right\rangle\!\right\rangle$ to the steady state is exhibited in Fig. 2.
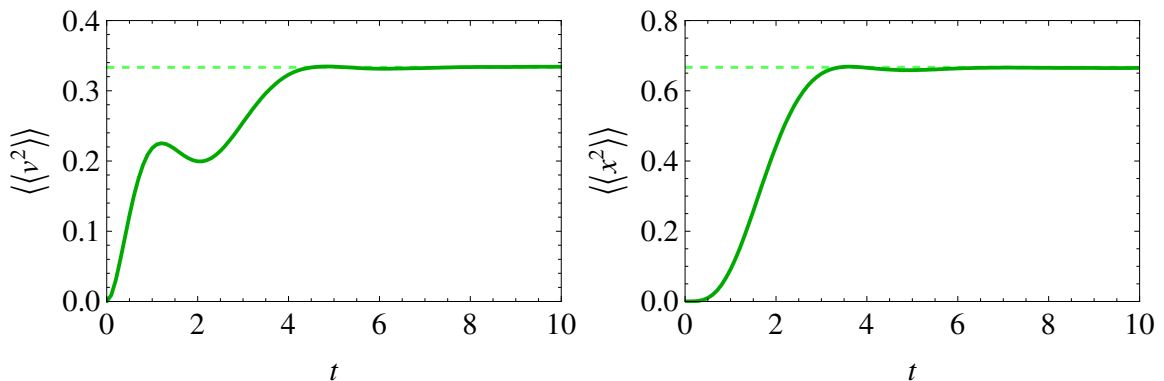
FIG. 2. Time evolution of $\left\langle\!\left\langle v^2 \right\rangle\!\right\rangle$ (left panel) and $\left\langle\!\left\langle x^2 \right\rangle\!\right\rangle$ (right panel). The full line corresponds to numerical results obtained com averages over 10^6 samples with: $m = k = \alpha = \gamma = 1$, $a = -b = 1$ and $\mu = \bar{\mu} = 1/2$. The dashed line represents the stationary state limit $\left\langle\!\left\langle v^2 \right\rangle\!\right\rangle = 1/3$ and $\left\langle\!\left\langle x^2 \right\rangle\!\right\rangle = 2/3$.

The definition of $\mathcal{T}$ is also important for understanding the statistics of the system as we change the rate μ, namely when it approaches the white-noise limit, $\mu \to \infty$

---

[1] Bear in mind that the white-noise limit of the telegraph noise is not the Gaussian though.

(*i.e.*, $\alpha^{-1} \to 0$). If the temperature is kept constant as we change μ, the gap between amplitudes, Δ, should go as,

$$|\Delta| = \mathcal{T}^{\frac{1}{2}} \sqrt{\frac{\gamma \, \hat{\rho} \, [k + \hat{\rho} \, \mu \, (\gamma + m \, \hat{\rho} \, \mu)]}{m \, \mu \, \rho}} \tag{33}$$

$$\sim \mathcal{T}^{\frac{1}{2}} \mu^{1/2}.$$

Let us now look at higher-order cumulants that are equal to zero for Gaussian distributions, namely the third and the fourth which are crucial for characterising the distribution. The third order cumulant is defined as,

$$\langle\langle \mathcal{O}^3 \rangle\rangle = \langle \mathcal{O}^3 \rangle - 3 \langle\langle \mathcal{O}^2 \rangle\rangle \langle \mathcal{O} \rangle - \langle \mathcal{O} \rangle^3. \tag{34}$$

The calculations from Eq. (23) yield,[2]

$$\langle\langle v^3 \rangle\rangle = 2 \frac{\Delta^3 \alpha^2 \, p \, [1 + p \, (2 \, p - 3)] \, [3 \, k \, m - 2 \gamma \, \hat{\gamma}]}{\hat{\gamma} \, \hat{k} \, (2\gamma^2 + k \, m) \, [4 \, k + \alpha \, (\gamma + \hat{\gamma})]}. \tag{35}$$

for the velocity whereas for the position,

$$\langle\langle x^3 \rangle\rangle = 2 \frac{\Delta^3 \, P \, (2p - 1) \, [k \, m \, (5 \, \hat{\gamma} - 3\gamma) + 2 \, \hat{\gamma}^2 \, (\gamma + \hat{\gamma})]}{k \, \hat{\gamma} \, \hat{k} \, (k \, m + 2\gamma^2) \, [4 \, k + \alpha \, (\hat{\gamma} + \gamma)]}. \tag{36}$$

The convergence to the values of $\langle\langle v^3 \rangle\rangle$ and $\langle\langle x^3 \rangle\rangle$ is plotted in Fig. 3.

From Eqs. (35) and (36) we compute the skewness,

$$A_{\mathcal{O}} \equiv \frac{\langle\langle \mathcal{O}^3 \rangle\rangle}{\langle\langle \mathcal{O}^2 \rangle\rangle^{3/2}}.$$

Explicitly, we have for the velocity,

$$A_v = \frac{2 \, \gamma \, (2p - 1) \, [3 \, k \, m - 2 \, \gamma \, \hat{\gamma}]}{\hat{\gamma} \, (2\gamma^2 + k \, m) \, [4k + \alpha \, (\gamma + \hat{\gamma})]} \sqrt{\frac{\alpha \, \gamma^3 \, \hat{k}}{P}}, \tag{37}$$

and for the position,

$$A_x = 2 \frac{(2 \, p - 1) \, [k \, m \, (5 \, \hat{\gamma} - 3\gamma) + 2 \, \hat{\gamma}^2 \, (\hat{\gamma} + \gamma)]}{k \, \hat{\gamma} \, \hat{k} \, (k \, m + 2\gamma^2) \, [4 \, k + \alpha \, (\hat{\gamma} + \gamma)]} \sqrt{\frac{\alpha \, \gamma^3 k \, \hat{k}}{P \, \hat{\gamma}^5}}. \tag{38}$$

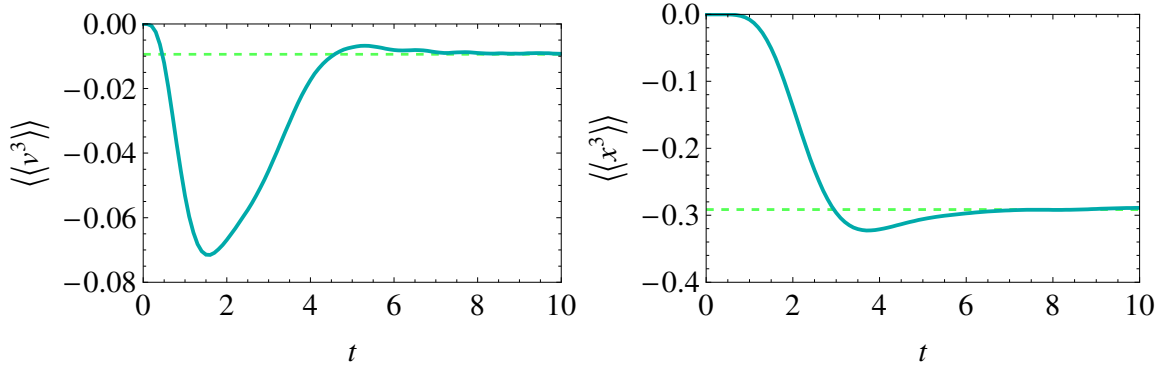[2] For the sake of simplicity we assume $\Delta > 0$.

FIG. 3.   Time evolution of $\langle\langle v^3 \rangle\rangle$ (left panel) and $\langle\langle x^3 \rangle\rangle$ (right panel). The full line corresponds to numerical results obtained com averages over 10^6 samples with: $m = k = \alpha = \gamma = 1$, $a = -b = 1$, $\mu = 2/3$, $\bar{\mu} = 1/3$. The dashed line represents the stationary state limit $\langle\langle v^3 \rangle\rangle = -16/1701 = 9.4 \times 10^{-3}$ and $\langle\langle x^3 \rangle\rangle = -479/1701 = -0.2915\ldots$.

Equation (37) allows learning that, for a fixed value of p, the skewness depends on the relation between the mechanical parameters and the colour of the noise. Explicitly, turning our attention to the behaviour of A_v as a function of the probability p, the skewness of the velocity would concur with the skewness of the telegraph noise: right-skewed when $p > 1/2$ and left-skewed when $p < 1/2$. However, the sign of A_v changes with the sign of $[3\,k\,m - 2\,\gamma\,\hat{\gamma}]$ as well. We explore this fact from different perspectives by finding critical values, $e.g.$, for α at which A_v changes sign,

$$\alpha^* = \max\left[\frac{3\,k}{2\,\gamma} - \frac{\gamma}{m}, 0\right]. \tag{39}$$

For $\alpha > \alpha^*$, the skewness is opposite to that given by p and the same otherwise. This critical behaviour can be expressed for the mechanical parameters as well,

$$k^* = \max\left[\frac{2\,\gamma\,(\gamma + m\,\alpha)}{3\,m}, 0\right] \qquad \text{or} \qquad \gamma^* = \max\left[\frac{\sqrt{m\,(6\,k + m\,\alpha^2)} - m\,\alpha}{2}, 0\right]. \tag{40}$$

In that case, for $k < k^*$ or $\gamma > \gamma^*$, the sign of A_v is contrary to the behaviour established by p. In order to provide some reasoning on this fact we center our attention on the dissipation taking place in the system. If the telegraph noise has uneven exchange rates ($\rho \neq 1$), we make one state of the noise to outweigh the other. If the system is due to achieve a stationary state, the prevalence of one of the states of the stochastic force

must be set off by the conservative force (created by the harmonic potential) — that is a function of the position and whose skewness is always the same as ζ — and the dissipative force. That said, depending on the limits established in Eqs. (39) and (40), it might be necessary to have an asymmetry that is complemmentary to the skweness of the noise. Because of the conservative nature of elastic force that effect must come from dissipation, which implies the change of the sign of A_v. In Fig. 4, we present the behaviour of the skewness for different values of α.
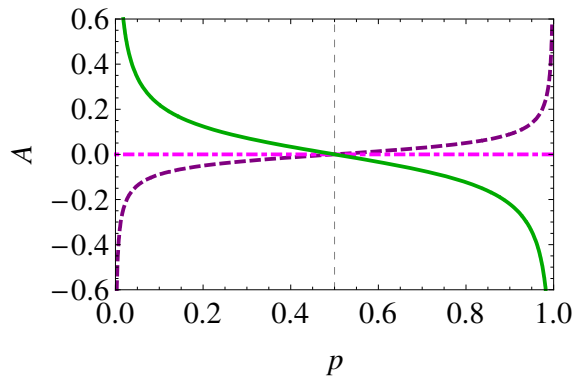
FIG. 4.   Asymmetry of $f(v)$ v probability p. For all the cases $m = k = \gamma = 1$, $a = -b = 1$. The green full line is for $\alpha = 1$, the purple dashed line is for $\alpha = 1/4$, and the magenta dotdashed line corresponds to $\alpha = \alpha^* = 1/2$ for which the asymmetry of the distribution changes sign in accordance with Eq. (39).

According to the theorem of the characteristic function by Marcinkiewicz [33], a probability density function either has two non-vanishing cumulants (and it is a Gaussian) or it must have an infinite set of non-vanishing cumulants[3]. Making *no assumptions* on the gap, Δ, and the ratio between jump rates, ρ, we make μ going to infinity, so that ζ approaches white noise. Fixing the Marconi temperature, we plug Eq. (33) into Eq. (35) to get,

$$\langle\langle v^3 \rangle\rangle \sim \mathcal{T}^{\frac{3}{2}}\frac{\mu^{5/2}}{\mu^3} \to 0 \qquad (\mu \to \infty). \tag{41}$$

Although the expressions for the other cumulants get more and more intricate, it is not difficult to understand that $\langle\langle v^n \rangle\rangle \sim \mu^{\frac{2-n}{2}}$ and the same for $\langle\langle x^n \rangle\rangle$ for $n \geq 3$. This

---

[3] Although for symmetric distributions all the odd cumulants zero out, one always have $\langle\langle \mathcal{O}^{2n} \rangle\rangle \neq 0$

($n \in \mathbb{N}$) for non-Gaussian distributions.

guarantees that the distributions $f(x)$ and $f(v)$ converge to the Gaussian as depicted in Fig. 6.

To conclude the statistical analysis of v and x, we have inspected the non-Gaussian nature of the respective distributions. This is best done using the kurtosis

$$C \equiv \frac{\langle\langle \mathcal{O}^4 \rangle\rangle}{\langle\langle \mathcal{O}^2 \rangle\rangle^2}, \tag{42}$$

instead of the fourth order cumulant. The results are the following: for the velocity,

$$C_v = 3\frac{\hat{k}\,[18\,m\,k^3\,\mathcal{F}_1 + 2\,k^2\,\mathcal{F}_2 + \alpha\,\hat{\gamma}\,k\,\mathcal{F}_2 + 3\alpha^2\gamma^2\,\hat{\gamma}^2(\hat{\gamma}+\gamma)\,\mathcal{F}_2]}{\hat{\gamma}\,P\,\alpha\,(3\gamma^2 + 4k\,m)\,[4k + \alpha(\hat{\gamma}+\gamma)]\,[km + \hat{\gamma}(\hat{\gamma}+\gamma)]\,[9k + \alpha(\hat{\gamma}+2\,\gamma)]} - 3 \tag{43}$$

and for the position,

$$C_x = 6\frac{k\,\gamma\,(\mathcal{G}_1 + k\,\hat{\gamma}\,\mathcal{G}_2 + 3k^3m^2\,\mathcal{G}_3 + k^2m\,\mathcal{G}_4)}{P\,\hat{\gamma}^3\left(3k + \hat{k}\right)(3\gamma^2 + 4km)\,[9k + \alpha\,(\hat{\gamma}+2\gamma)]\,[\delta_\gamma^2 + 3\gamma\delta_\gamma + 2\gamma^2 + km]}, \tag{44}$$

where the functions $\mathcal{F}$ and $\mathcal{G}$ are made explicit in B.

The kurtosis of the position is always negative, *i.e.*, the distribution is platykurtic (sub-Gaussian). Contrarily, the kurtosis of the velocity is positive (leptokurtic) for small values of α and for large values it goes to zero from below. This means that looking in the $C_v - p$ plane (α is a parameter), there is a critical value of the colour, $\alpha^\dagger$, for which the distribution $p(v)$ is mesokurtic for $p^\dagger = p^\ddagger = 1/2$ but non-Gaussian though, as Fig. 6 let us understand. From there on, the distribution of velocities has two leptokurtic regions for $p < p^\dagger$ e $p > p^\ddagger = p^\dagger + 1/2$ and is platykurtic elsewhere.

For large values of α, the form of the distributions $f(x)$ and $f(v)$ can be understood as follows: when the exchange rates μ and $\bar{\mu}$ are very large but smaller than the relaxation rate γ/m, we can solve the dynamical equation for the time spell equal to m/γ assuming a fixed value for ζ. Therefore, the solution to the equation of motion with initial conditions $x(t=0) = 0$ and $v(t=0) = 0$, reads,

$$x(t) = -\frac{\zeta}{k} + \exp\left[-\frac{t}{2\,\tau_r}\right]\left\{\frac{\zeta}{k}\cos[2\,\Omega\,t] + \frac{\gamma\,\zeta}{k\sqrt{4\,k\,m - \gamma^2}}\sin[2\,\Omega\,t]\right\}. \tag{45}$$

In this scenario, the system tends to dwell closer to $-a/k$ and $-b/k$. This explains the peaks in Fig. 6 (left panel) around $x = \pm 1$ which are more pronounced, the larger the difference between τ_r and the scales μ^{-1} and $\bar{\mu}^{-1}$. The same difference in the scales

explains the strong peak around $v = 0$ (right panel). Regarding the U-shape between the peaks in the left panel they are the outcome of the (damping) oscillatory terms. It is worth remembering that the probability density function of a trigonometric variable, $\mathcal{O}$, is,

$$f(\mathcal{O}) = \frac{1}{\pi\sqrt{1 - \mathcal{O}^2}}. \tag{46}$$

As the two scales concur, the distribution approaches a bell-shape to match the Gaussian in the white-noise limit. The steady state solution for the overdamped case and specific noise features can be found in [30, 31].
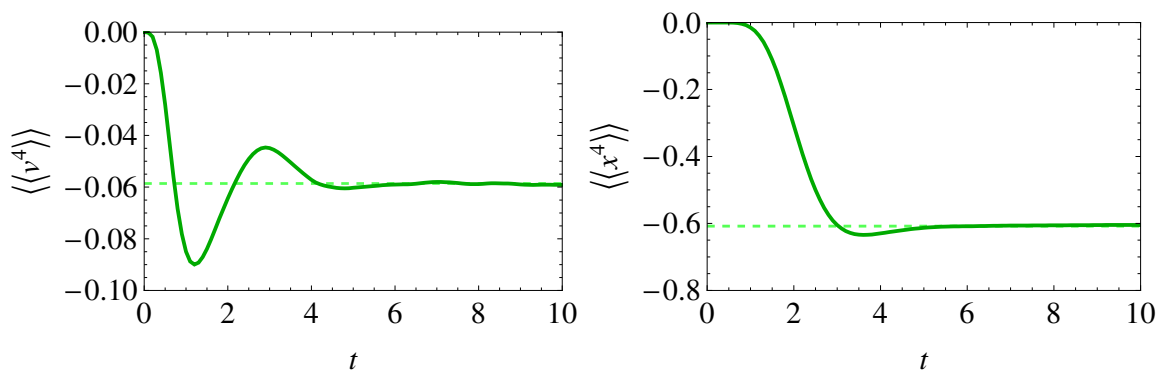

FIG. 5. Time evolution of $\langle\langle v^4 \rangle\rangle$ (left panel) and $\langle\langle x^4 \rangle\rangle$ (right panel). The full line corresponds to results obtained by numerical simulation averaged over 10^6 samples with: $m = k = \alpha = \gamma = 1$, $a = -b = 1$ e $\mu = \bar{\mu} = 1/2$. The dashed line represents the asymptotic stationary state value $\langle\langle v^4 \rangle\rangle = -16/273 = -0.0586\ldots$ (left panel) and $\langle\langle v^4 \rangle\rangle = -166/273 = -0.608\ldots$.

IV. ENERGETIC CONSIDERATIONS

Looking at the dynamical equations, the change in the energy of the particle is the outcome of the superposition of the the dissipative force,

$$F_{\text{dis}}(t) = -\gamma\, v(t), \tag{47}$$

which performs negative work, and the stochastic force that is the sole responsible for injecting energy into the system,
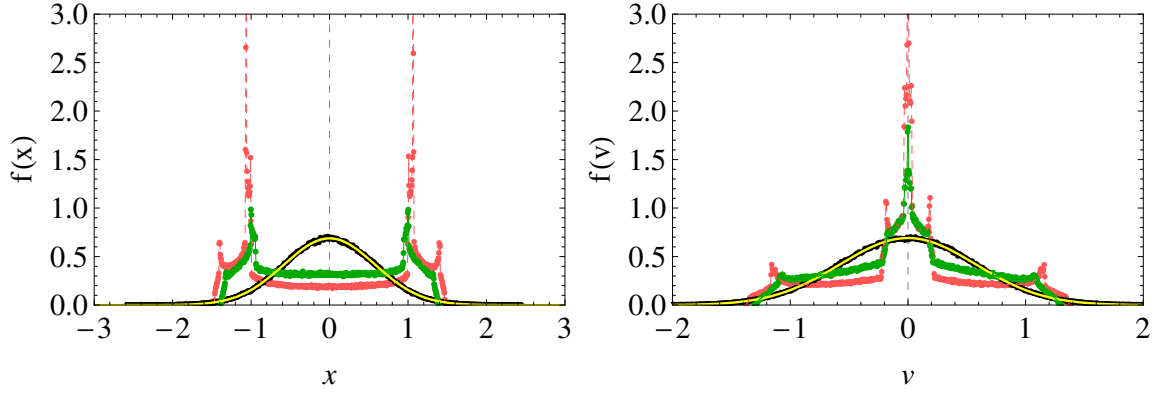
$$F_{\text{inj}}(t) = \zeta(t). \tag{48}$$

FIG. 6.   Stationary distribution $f(v)$ v v (left panel) and stationary distribution $f(x)$ v x (right panel) obtained by numerical simulation. For all cases, $T = 1/3$, $m = k = \gamma = 1$, $p = \bar{p} = 1/2$ e $b = -a$. The legend goes as follows: $\{\alpha = 1, a = 1\}$ (green); $\left\{\alpha = \alpha^\dagger = 0.5438\ldots, a = 1.06188\ldots\right\}$ (red) and $\left\{\alpha = 100, a = \sqrt{3367/100}\right\}$ (black). The yellow line represents a Gaussian with variance equal to $1/3$ (left panel) and $2/3$ (right panel), that corresponds to the asymptotic limits of $p(v)$ and $p(x)$ when α approaches infinity.
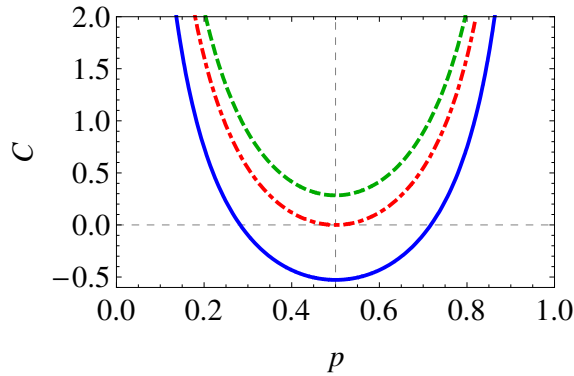

FIG. 7.   Kurtosis of the velocity v p with $m = k = \gamma = 1$ e $b = -a = 1$. The green line corresponds to $\alpha = 1$, the dotdashed red line is for $\alpha = \alpha^\dagger = 0.5438\ldots$ and the dashed blue line $\alpha = 45/100$.

Putting it mathematically, the total energy change, *i.e.*, variation of kinetic energy, K, plus the variation of potential energy, V, between initial time $t_0 = 0$ and some instant
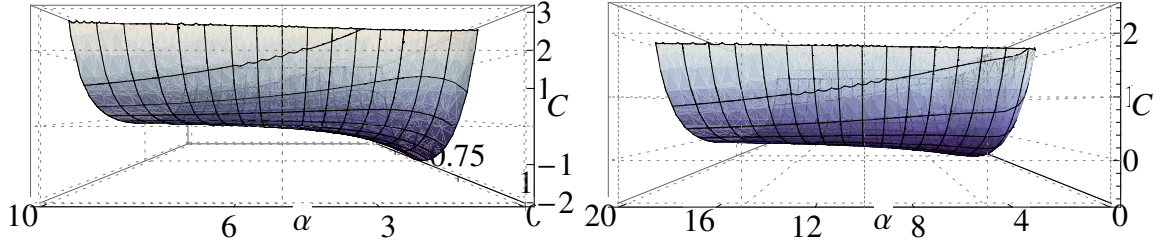
FIG. 8.   Kurtosis of the the position (left panel) and velocity (right panel) as a function of α and p $m = k = \gamma = 1$ e $b = -a = 1$.

$t = \Xi$ is given by,

$$E\left(\Xi\right) \equiv K\left(\Xi\right) + V\left(\Xi\right) = \int_0^\Xi \left[-\gamma\, v\left(t\right)\right] v\left(t\right)\, dt + \int_0^\Xi \zeta\left(t\right) v\left(t\right)\, dt$$

(49)

$$= J_{\mathrm{dis}}\left(\Xi\right) + J_{\mathrm{inj}}\left(\Xi\right).$$

where we define J as the energy fluxes, which are stochastic processes as well. In the present work, we are only interested in their long term behaviour so that Ξ is much larger than both m/γ and α^{-1}. At that stage, the energy injected by the (work) reservoir must be set off by the dissipation the flux of which corresponds to heat. As a matter of fact, all the absolute values of the statistical moments/cumulants of the fluxes $J_{\mathrm{inj}}\left(\Xi\right)$ and $J_{\mathrm{dis}}\left(\Xi\right)$ will match.

Resorting to our Fourier-Laplace method the moments of each flux are obtained from,

$$\left\langle J_{\mathrm{inj}}^n\left(\Xi\right)\right\rangle = \prod_{l=1}^n \int_0^\Xi dt_l \int \frac{dq_{2l-1}}{2\pi}\frac{dq_{2l}}{2\pi} \mathrm{e}^{[(\mathrm{i}\, q_{2l-1} + \mathrm{i}\, q_{2l} + 2\,\varepsilon) t_l]} \frac{(\mathrm{i}\, q_{2l} + \varepsilon)}{R\left(\mathrm{i}\, q_{2l} + \varepsilon\right)}$$

(50)

$$\times \left\langle \prod_{l=1}^n \tilde{\zeta}\left(\mathrm{i}\, q_{2l-1} + \varepsilon\right) \tilde{\zeta}\left(\mathrm{i}\, q_{2l} + \varepsilon\right)\right\rangle,$$

and,

$$\left\langle J_{\mathrm{dis}}^n\left(\Xi\right)\right\rangle = \prod_{l=1}^n \left(-\gamma\right) \int_0^\Xi dt_l \int \frac{dq_{2l-1}}{2\pi}\frac{dq_{2l}}{2\pi} \mathrm{e}^{[(\mathrm{i}\, q_{2l-1} + \mathrm{i}\, q_{2l} + 2\,\varepsilon) t_l]} \frac{(\mathrm{i}\, q_{2l-1} + \varepsilon)}{R\left(\mathrm{i}\, q_{2l-1} + \varepsilon\right)} \frac{(\mathrm{i}\, q_{2l} + \varepsilon)}{R\left(\mathrm{i}\, q_{2l} + \varepsilon\right)}$$

$$\times \left\langle \prod_{l=1}^n \tilde{\zeta}\left(\mathrm{i}\, q_{2l-1} + \varepsilon\right) \tilde{\zeta}\left(\mathrm{i}\, q_{2l} + \varepsilon\right)\right\rangle.$$

(51)

Once again, the result depends on the moment $\left\langle \prod_{l=1}^n \tilde{\zeta}\left(\mathrm{i}\, q_{2l-1} + \varepsilon\right) \tilde{\zeta}\left(\mathrm{i}\, q_{2l} + \varepsilon\right)\right\rangle$, but for the injected flux the noise factors $\tilde{\zeta}$ have different origins. In other words, for
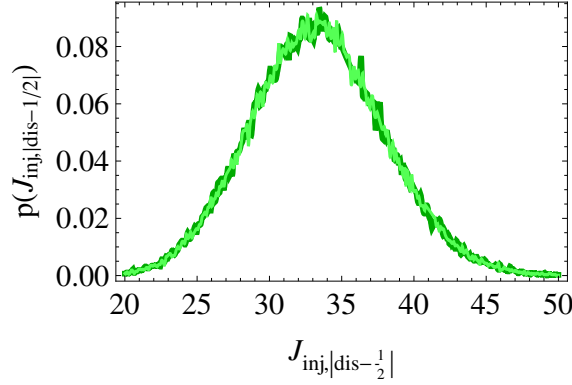
FIG. 9. Probability density function of $J_{\text{inj}}(\Xi)$ e $J_{|\text{dis}|}(\Xi)$ obtained by numerical simulation with $m = k = \alpha = \gamma = 1$, $a = -b = 1$, $\mu = \bar{\mu} = 1/2$ e $\Xi = 1000$. It is visible that the two distributions match. We have shifted of $1/2$ in the dissipated flux is made to balance out the constant terms (linked to the transient) that do not appear in the calculation of J_{dis}.

$\left\langle \prod_{l=1}^{n} \tilde{\zeta}\left(\mathrm{i}\, q_{2l-1} + \varepsilon\right) \tilde{\zeta}\left(\mathrm{i}\, q_{2l} + \varepsilon\right) \right\rangle_{\text{inj}}$, there are $(2n)!$ possible arrangements; however, we can only benefit from the indistinguishability between pairs of terms and thus the total number of equal terms amounts to $n!$. On the other hand, for the dissipative flux, the degeneracy is equal to $2^n n!$ because the noises $\tilde{\zeta}\left(\mathrm{i}\, q_{2l-1} + \varepsilon\right)$ and $\tilde{\zeta}\left(\mathrm{i}\, q_{2l} + \varepsilon\right)$ can be swapped without changing the result.

We define the long term cumulants as,

$$\langle\langle \mathcal{J}^n (\Xi) \rangle\rangle \equiv \Xi \lim_{t \to \infty} \frac{1}{t} \langle\langle J^n (t) \rangle\rangle \tag{52}$$
$$= \Xi \, r_{\langle\langle \mathcal{J}^n(\Xi) \rangle\rangle},$$

and $r_{\langle\langle \mathcal{J}^n(\Xi) \rangle\rangle}$ the respective growth rate.

Using Eq. (50) and (51), we have for the full average fluxes,

$$\langle J_{\text{inj}}(\Xi) \rangle = \frac{\gamma \mathcal{T}}{m} \Xi + \left[\frac{\Delta^2 P}{\hat{k}} (k - \alpha\, \delta_\gamma) + \frac{(a\, p + b\, \bar{p})^2}{k} \right]$$

$$\tag{53}$$

$$= \frac{\gamma \mathcal{T}}{m} \Xi + E_{\text{inj}},$$

and,

$$\langle J_{\text{dis}}\,(\Xi) \rangle = -\frac{\gamma \mathcal{T}}{m}\,\Xi + \left\{ \frac{\Delta^2 P}{\gamma\,\hat{k}^2}\left[k\,(2\,\hat{\gamma} - \gamma) + \alpha\,\left(2\,\hat{\gamma}^2 - 2\gamma^2 + \gamma\,\hat{\gamma} \right) \right] - \frac{(a\,p + b\,\bar{p})^2}{2\,k} \right\}$$

$$\tag{54}$$

$$= -\frac{\gamma \mathcal{T}}{m}\,\Xi + E_{\text{dis}}.$$

Therefrom, we identify,

$$\langle \mathcal{J}_{\text{inj}}\,(\Xi) \rangle = |\langle \mathcal{J}_{\text{dis}}\,(\Xi) \rangle| = \frac{\gamma \mathcal{T}}{m}\,\Xi. \tag{55}$$

Moreover, adding the time independent terms we find,

$$E_{\text{inj}} + E_{\text{dis}} = \frac{m}{2}\frac{\Delta^2\,P\,\alpha}{\hat{k}} + \frac{\Delta^2\,P\,\hat{\gamma}}{2\,\gamma\,\hat{k}} + \frac{(a\,p + b\,\bar{p})^2}{2\,k}$$

$$\tag{56}$$

$$= \frac{1}{2}\,m\,\langle v^2 \rangle + \frac{1}{2}\,k\,\langle\langle x^2 \rangle\rangle + \frac{1}{2}\,k\,\langle x \rangle^2,$$

whence we identify the kinetic energy of the stationary state in the first term whereas the second and third terms correspond to the potential energy. The third term is only non-vanishing if the noise is not balanced ($a\,p \neq -\,b\,\bar{p}$) and emerges from the fact that in such conditions the average position is different from the minimum of the potential for which there is an energy cost. In Fig. 10 (left panel), we plot the time evolution of the average fluxes with time Ξ. For large Ξ, the difference between the lines (the sum of the fluxes) remains constant and corresponds to the total energy of the particle. It is worth referring that this case differs from the thermal reservoir system since the (average) total energy does not totally emerge from the dissipative term.

Since the results are equivalent, we will use the dissipation flux to compute the variance because it has a larger degeneracy. For the second order moment we have 3 different terms, each one with a degeneracy number equal to 16. Subtracting $\langle J_{\text{dis}}\,(\Xi) \rangle^2$ to $\langle J_{\text{dis}}^2\,(\Xi) \rangle$ we have the second order cumulant,

$$\langle\langle \mathcal{J}^2\,(\Xi) \rangle\rangle = \frac{P\,\alpha\,[a^4\mathcal{H}_{11} + 2\,a\,b\,(a^2\mathcal{H}_{12} + b^2\mathcal{H}_{13}) + a^2 b^2\,(\mathcal{H}_{14} + \mathcal{H}_{15}) + b^4\,\mathcal{H}_{16}]}{4\,k\,\hat{k}^3}\,\Xi \tag{57}$$

$$+ \frac{a^4 p\,\mathcal{H}_{21} + 4\,a\,b\,P\,\alpha\,(a^2\mathcal{H}_{22} + b^2\mathcal{H}_{23}) + 2a^2 b^2\,P\,(\mathcal{H}_{24} + \alpha^2\mathcal{H}_{25}) + b^4\bar{p}\,\mathcal{H}_{26}}{k\,\gamma\,\hat{\gamma}\,\hat{k}\,[4k + \alpha(\hat{\gamma} + \gamma)]}\,\Xi$$

$$+ \frac{a^4 p\,\mathcal{H}_{31} + 4\,a\,b\,P\,\alpha\,(a^2\mathcal{H}_{32} + b^2\mathcal{H}_{33}) + 2a^2 b^2\,P\,(\mathcal{H}_{34} + \alpha^2\mathcal{H}_{35}) + b^4\bar{p}\,\mathcal{H}_{36}}{k\,\alpha\,\gamma\,\hat{k}\,\left(\gamma^2 - \delta_\gamma^2 + 4\,k\,m \right)}\,\Xi,$$
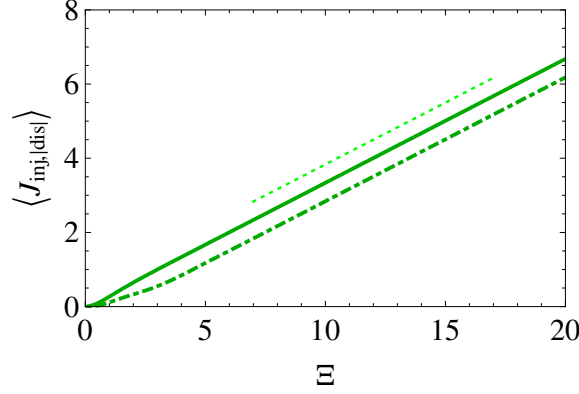
FIG. 10. Time evolution of the average fluxes $\langle J_{\text{inj}}(\Xi)\rangle$ (full line) and $|\langle J_{\text{dis}}(\Xi)\rangle|$ (dotdashed line) obtained by numerical simulation of 10^6 samples with $m = k = \alpha = \gamma = 1$, $a = -b = 1$, $\mu = \bar{\mu} = 1/2$. The dotted line represents the asymptotic growth given by Eq. (55), $\langle \mathcal{J}(\Xi)\rangle = \Xi/3$.
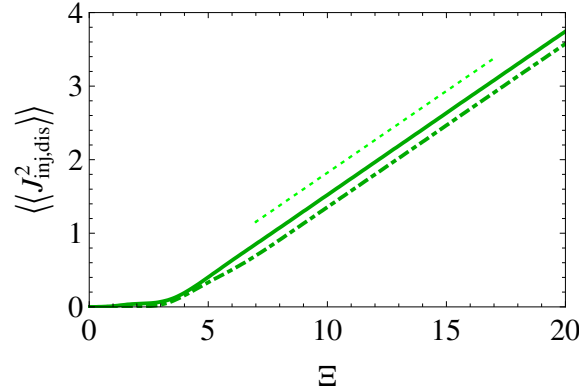

FIG. 11. Time Evolution of the variance of the fluxes $\left\langle\left\langle J_{\text{inj}}^2(\Xi)\right\rangle\right\rangle$ (full line) and $\left\langle\left\langle J_{\text{dis}}^2(\Xi)\right\rangle\right\rangle$ (dotdashed line) obtained by numerical simulation of 10^6 samples with $m = k = \alpha = \gamma = 1$, $a = -b = 1$, $\mu = \bar{\mu} = 1/2$. The dotted line has got a slope equal to $8/36 = 0.2\,(2)$ as given by Eq. (57).

with the functions $\mathcal{H}_{ij}$ as defined in the appendix.

In Fig. 11, we show the comparison between results from numerical simulation and Eq. (57).

As our calculations demonstrate, the higher the order of the cumulant $\langle\langle\mathcal{J}^n(\Xi)\rangle\rangle$, the
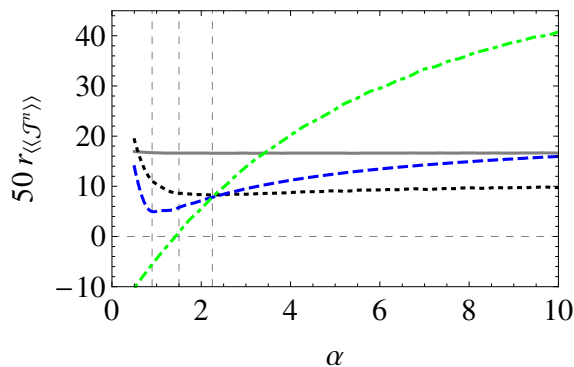
FIG. 12. Cumulants of the fluxes, $\langle\langle\mathcal{J}^n(\Xi)\rangle\rangle$, as a function of the colour of the telegraph noise obtained by numerical simulation with $m = k = \gamma = 1$, $a = -b = 1$ and Marconi temeprature $1/3$. The legend goes as follows: full grey line - average; dotted black line - variance; blue dashed line - $3th$ order cumulant; dotdashed green line the $4th$ order cumulant. The $\langle\langle\mathcal{J}^n(\Xi)\rangle\rangle$ has a minimum located at $\alpha \simeq 1.05$. For $\alpha \simeq 1.5$ the distribution changes its kurtosis going from platykurtic to a leptokurtic.

more intricate the analytical expressions get. Using our method these expression can be precisely obtained; however due to their extension they are ever harder to understand regarding its physical content. To circumvent this snag we carried out numerical simulations to compute the slopes of each cumulant $\langle\langle\mathcal{J}^n(\Xi)\rangle\rangle$ with $n = \{3, 4\}$. These results allow enhancing an approximative approach based on the Edgeworth expansion to the probability distribution of $\mathcal{J}$, $\mathcal{L}(\mathcal{J})$, that can be seen as a large deviation of the injected/dissipated power. The evolution of the first four cumulants of the flux with α (for a fixed Marconi temperature) is presented in Fig. 12. For those numerical simulation results, we found out that the cumulant rates are very well described by,

$$r_{\langle\langle\mathcal{J}^3(\Xi)\rangle\rangle} = \frac{1}{50}\left[27.78 + 1.78\left(\frac{2.03}{\alpha}\right)^{1.89} - 22.14\left(\frac{2.03}{\alpha}\right)^{0.4}\right],$$

$$\tag{58}$$

$$r_{\langle\langle\mathcal{J}^4(\Xi)\rangle\rangle} = \frac{1}{50}\left[-17.04 + 14.05\,\alpha - 1.54\,\alpha^2 + 0.098\,\alpha^3 - 0.0027\,\alpha^4\right].$$

The curves in Fig. 12 show that the rate of the second order cumulant rapidly approaches its white-noise asymptotic limit. The skewness is always positive, but it has a minimum for $\alpha \simeq 1.05$ before going to white-noise limit. On the other hand, the Gaus-

sianity of the distribution changes its nature with the rate α; explicitly, for $\alpha < \alpha^* \simeq 1.41$, $\mathcal{L}(\mathcal{J})$ is platykurtic and leptokurtic otherwise. Heed that although for $\alpha = \alpha^*$ the large deviation function $\mathcal{L}(\mathcal{J})$ is mesokurtic it is still non-Gaussian. In other words, the white-noise limit of the large deviation function $\mathcal{L}(\mathcal{J})$ is not a Gaussian similarly to the thermal case. In latter case we have,

$$\mathcal{L}(\mathcal{J}) \sim \exp\left[-\frac{\left(\mathcal{J} - \frac{\gamma T}{m}\Xi\right)^2}{4\,T\,\mathcal{J}}\right].\tag{59}$$

V. FINAL REMARKS

In this manuscript, we carried out a thermostatistical study of a linear mechanical system with mass m subject to confinement, dissipation and a stochastic dichotomous force that we understood as the action of an athermal external (work) reservoir; external for the fluctuations and the dissipation do not have the same origin and therefore the fluctuation-dissipation relation is not verified. That description fits important nanomechanical phenomena like intracellular bidirectional transport on cytoskeletal filaments mediated by two sets of molecular motors, the kinetics of protein markers in capillary media among other types of problems. Because of its coloured nature, the telegraph noise used to represent the dichotomous force lies in a different class of stochastic processes other than the Lévy-Itô. In the latter, every white-noise stochastic process can be represented by a superposition of continuous (Brownian) and singular (Poissonian) measures. This means that Fokker-Planck methods are unfit for an accurate analysis of such systems as previous studies had proven. Treating the problem in Fourier-Laplace space, we were able to develop a statistical description of the position and velocity imposing no condition on the damping nature as well as symmetry properties of the noise, contrarily to the state of the art.

Regarding a stationary state analysis, we found that the position always presents the same qualitative properties as the telegraph noise regarding the skewness and the kurtosis. Differently, depending on the set of mechanical parameters of the system, the skewness of $f(v)$ can be opposed to that of the noise. This change in the skewness can be comprehended as follows: when the noise is unbalanced, $a\,p \neq b\,\bar{p}$, there must be some emerging feature of the system that compensates the prevalence of one of the sides of the noise;

taking into account that the confining force is conservative — and the sign of the skewness of the distribution $f(x)$ does not depend on the mechanical features of the system — the balance can only come from dissipation that is ruled by the velocity which then assumes an opposite skewness to the noise. With respect to the kurtosis the distribution $f(v)$ is leptokurtic for small values of α, $i.e.$, large waiting time between changes in the value of the noise, whereas $f(x)$ is always platykurtic.

From the second order moment of the velocity, we defined an effective temperature of the system (the Marconi temperature), which plays the role of typical scale of energy of a bi-modal particle. Nonetheless, due to the coloured nature of the noise, the equipartition of the energy does not hold and thus $\mathcal{V} = k\,x^2/2 \neq T/2$. That equality is only observed in the white-noise limit.

Afterwards, since in our analytical procedure we can skip making the propagator explicit, we were able to determine the statistics of time dependent quantities as well, namely the total energy fluxes (dissipated and injected), $\mathcal{J}$, that correspond to the large deviation of the respective powers. Analysing the behaviour of the respective large deviation function, $\mathcal{L}(\mathcal{J})$, we found that its variance converges fast to the asymptotic white-noise value. Moreover, the function $\mathcal{L}(\mathcal{J})$ can have different types of non-Gaussianity, $i.e.$, it is platykurtic for small jump rates of the noise and gets leptokurtic as the jump rate between states soars.

Last, despite of the fact that we are treating an athermal problem, we recall the existence of an effective temperature for this system and we look at the entropy production that ought to be related to the dissipated and injected fluxes. If the system attains a steady state, then the condition between the total entropy, S, the entropy production, Π, and entropy exchange, Ψ, is,

$$\frac{dS}{dt} = \Pi - \Psi = 0 \qquad\qquad (t \gg m/\gamma). \qquad\qquad (60)$$

Bearing in mind our results we bridge Π with $\mathcal{J}_{\text{inj}}$ and Ψ with $\mathcal{J}_{\text{dis}}$. Accordingly, from dimensional analysis, the energy flux up to some time t is the product of [entropy] by [temperature]. If we assume that the effective temperature of the bi-modal particle is the Marconi temperature, then we can easily verify that $\Pi = \Psi = \gamma/m$, exactly the same form obtained for linear systems in contact with reservoirs which fit the Lévy-Itô conditions. Therefore, the Marconi temperature is the energy scale that retrieves a universal form of

long-term entropy production/exchange.

The present analysis can be further expanded along different lines. In a purely thermostatistical perspective, we can consider a memory kernel for the dissipative term (with same spectrum as the noise α) so that the dichotomous work reservoir noise is analogue to a thermal internal reservoir as described by Kubo and Mori [34]. In this case, we expect to be capable of establishing an athermal fluctuation-dissipation relation and analyse the large deviations of the energy fluxes as well as fluctuation relations for work and entropy. In recent work of one of us it was shown the relevance of non-linearities in the confining potential when the reservoir is athermal (white-shot-noise), namely in the activation of higher-order cumulants that will act as sources of energy of higher order [12]; accordingly, it would be interesting to assess the impact of non-linearities (either in the confining potential or the dissipation) along the lines of the current manuscript and the points we have discussed. These studies can be made considering single or multiple particle systems in contact with different reservoirs.

As the present work evinces, the concept of temperature can be interpreted in a broader sense than that Thermodynamics imposes. On that account, several thermostatistical concepts can be recast taking into consideration the idiosyncrasies of the system. This works for both physical problems like superconducting systems where the uncertainty in the location of the vortices can be read as an effective temperature [35] and non-physical problems like a financial market for which the volatility also fits a temperature concept, which recently led the analysis of price dynamics to a internal reservoir approach [36]. Notwithstanding, especially at very short time scales, trading is more similar to a tug-of-war between buyers and sellers than a particle in a medium. In other words, for a high-frequency dynamics, one verifies that the price soars and drops very closely to a telegraph noise process. For little liquid markets, this feature jointly with periods without activity is even clearer. Therefore an appropriate analytical description would be a scenario consistent with a three-state noise for which we can perform a similar analysis.

ACKNOWLEDGMENTS

Appendix A: The telegraph noise

The telegraph noise, also known as dichotomous or 2-state Brownian noise, corresponds to a stochastic process $\{\zeta_t\}$ that assumes two values $\zeta = \{a, b\}$. In time, the noise switches from once state to the other according to pre-established (average) rates:

- μ when going from b to a;

- $\bar{\mu} = \rho\,\mu$ otherwise,

which yields the following master equation,

$$
\begin{cases}
\frac{\partial\, f(a,t\,|\,\zeta_0,t_0)}{\partial t} = \mu\, f\,(b,t\,|\,\zeta_0,t_0) - \bar{\mu}\, f\,(a,t\,|\,\zeta_0,t_0) \\[2ex]
\frac{\partial\, f(b,t\,|\,\zeta_0,t_0)}{\partial t} = \bar{\mu}\, f\,(a,t\,|\,\zeta_0,t_0) - \mu\, f\,(b,t\,|\,\zeta_0,t_0)
\end{cases}, \tag{A1}
$$

where $f\,(a,t\,|\,\zeta_0,t_0) + f\,(b,t\,|\,\zeta_0,t_0) = 1$. Assuming always the same initial condition,

$$
f\,(\zeta,t_0\,|\,\zeta_0,t_0) = \delta_{\zeta,\zeta_0}. \tag{A2}
$$

the solution to Eq. (A1) reads,

$$
\begin{cases}
f\,(a,t\,|\,\zeta_0,t_0) = p + \exp\left[-\alpha\,(t-t_0)\right]\,(\bar{p}\,\delta_{a,\zeta_0} - p\,\delta_{b,\zeta_0}) \\[2ex]
f\,(b,t\,|\,\zeta_0,t_0) = \bar{p} - \bar{p}\,\exp\left[-\alpha\,(t-t_0)\right]\,(\bar{p}\,\delta_{a,\zeta_0} - p\,\delta_{b,\zeta_0})
\end{cases}. \tag{A3}
$$

For long enough time intervals, $i.e.$, $t - t_0 \gg \alpha^{-1}$, the stationary distribution reads,

$$
f_{\text{est}}\,(\zeta) = p\,\delta_{a,\zeta} + \bar{p}\,\delta_{b,\zeta}. \tag{A4}
$$

From Eq. (A3) one determines the evolution of the noise between to instants t and t',

$$
f\,(a,t\,|\,a,t') = p + \bar{p}\,\mathrm{e}^{-\alpha(t-t')}, \quad f\,(a,t\,|\,b,t') = p - p\,\mathrm{e}^{-\alpha(t-t')},
$$

$$
\tag{A5}
$$

$$
f\,(b,t\,|\,a,t') = \bar{p} - \bar{p}\,\mathrm{e}^{-\alpha(t-t')}, \quad f\,(b,t\,|\,b,t') = \bar{p} + p\,\mathrm{e}^{-\alpha(t-t')}.
$$

Still from the master equation it is possible to determine the moments of n-th order of telegraph noise,

$$\langle \zeta(t_1) \ldots \zeta(t_n) \rangle = \sum_{\substack{\zeta(t_1),\ldots,\zeta(t_n) \\ (t_1 > \ldots > t_n)}} [\zeta(t_1) \ldots \zeta(t_n)] \, p(\zeta(t_1), \ldots, \zeta(t_n))$$

(A6)

$$= \sum_{\zeta(t_1),\ldots,\zeta(t_n)} [\zeta(t_1) \ldots \zeta(t_n)] \, p[\zeta(t_1)|\zeta(t_2)] \ldots p[\zeta(t_{n-1})|\zeta(t_n)] \, p[\zeta(t_n)].$$

Notice that when computing the general expressions for the moments of n-th order we must include all time orderings.

Regarding the second order cumulant,

$$\langle \zeta(t_1) \, \zeta(t_2) \rangle_c = \langle \zeta(t_1) \, \zeta(t_2) \rangle - \langle \zeta(t_1) \rangle \langle \zeta(t_2) \rangle$$

(A7)

$$= \Delta^2 \left[P \, \mathrm{e}^{-\alpha|t_1 - t_2|} - \bar{p}^2 \, \mathrm{e}^{-\alpha(t_1 + t_2)} \right] - \Delta \, \langle \zeta \rangle \, \bar{p} \left(\mathrm{e}^{-\alpha t_1} + \mathrm{e}^{-\alpha t_2} \right).$$

In the long time limit,

$$\langle \zeta(t_1) \, \zeta(t_2) \rangle_c = \Delta^2 \, P \, \mathrm{e}^{-\alpha|t_1 - t_2|} \tag{A8}$$

$$= \mathcal{B} \, \mathcal{D} \, \mathrm{e}^{-\alpha|t_1 - t_2|},$$

where,

$$\mathcal{A} = a \, p + b \, \bar{p}, \quad \mathcal{B} = (a - b) \, p, \quad \mathcal{D} = (a - b) \, \bar{p}. \tag{A9}$$

It is worth recalling that maintaining the amplitudes of both states, i.e., keeping Δ constant, and increasing the frequency of the noise ($\alpha \to \infty$), the correlation $\langle \zeta(t_1) \, \zeta(t_2) \rangle_c$ would vanish, which does not correspond to the coloured gaussian noise case.

1. Numerical implementation of the noise

In order to assess our analytical results and carry out further numerical analysis (for which analytical analysis are quite complex and physically dim). In that case two options occur:

I.: Looking to Eq. (A3) and assuming a given initial condition, x_0, one analyses the probability that the noise has a value x at time t, comparing $f(x, t \mid x_0, t_0)$ with a random number, r, uniformly distributed between 0 and 1. If $f(x, t \mid x_0, t_0) > r$ the noise gets the value x. This check is made a some (fixed) time interval Δ_t that should be adjusted according to the smallest scale the parameters impose.

II.: Another method is based on the first passage process and corresponds to the numerical method we employed. In that case, the master Equation is solved taking into account an extra condition,

$$
\begin{cases}
f(b, t \mid a, t_0) = 0 \impliedby x_0 = a \\
\\
f(a, t \mid b, t_0) = 0 \impliedby x_0 = b
\end{cases}
. \tag{A10}
$$

The respective solution implies that the probability the noise changes from a to b after an interval of time $\delta_t = t - t_0$ is equal to,

$$
Q_{a \to b}(\delta_t) = \bar{\mu} \, \exp\left[-\bar{\mu} \, \delta_t\right], \tag{A11}
$$

and the probability the noise switches from b to a after $\delta_t = t - t_0$,

$$
Q_{b \to a}(\delta_t) = \mu \, \exp\left[-\mu \, \delta_t\right]. \tag{A12}
$$

If the noise is equal to a (b) at instant t_0, we pick a number, δ_t, exponentially distributed with characteristic scale $\bar{\mu}^{-1}$ (μ^{-1}); the noise keeps its value a (b) and at instant $t_0 + \delta_t = t$ it assumes a new value b (a). Then, for computational effects t turns into the new initial time and a new waiting time δ_t is computed and so forth.

: In our case, we assume $\xi(t_0) = a$.

Appendix B: Explicit forms of the functions $\mathcal{F}$, $\mathcal{G}$, and $\mathcal{H}$

In these functions we have the following simplified expressions,

$$
\delta_\gamma \equiv \hat{\gamma} - \gamma, \qquad \delta_p \equiv \bar{p} - p.
$$

1. Functions for Eq. (43)

$$\mathcal{F}_1 = \gamma^2 + 3\gamma\delta_\gamma + 8\,P\,\delta_\gamma^2,$$

$$\mathcal{F}_2 = 18\,\gamma^4 + 47\,\gamma^3\,\delta_\gamma + 63\,(1-P\,)\,\gamma^2\,\delta_\gamma^2$$
$$+3\,(10-7P)\,\gamma\,\delta_\gamma^3 + 26\,P\delta_\gamma^4,$$

$$\mathcal{F}_3 = 24\gamma^4 + 2\,(7-57P\,)\,\gamma^3\,\delta_\gamma + (65P+6)\,\gamma^2\,\delta_\gamma^2$$
$$+2\,(3-P)\,\gamma\,\delta_\gamma^3 + 4\,P\,\delta_\gamma^4,$$

$$\mathcal{F}_4 = (2-6P)\,\gamma + P\delta_\gamma.$$

(B1)

2. Functions for Eq. (44)

$$\mathcal{G}_1 = 3\,(5P+1)\,\alpha\,\hat{\gamma}^4(\hat{\gamma}+\gamma)^2(\hat{\gamma}+2\gamma),$$

$$\mathcal{G}_2 = (170P+33)\,\delta_\gamma^5 + 10\,(110P+21)\,\gamma\,\delta_\gamma^4 + (2411P+445)\,\gamma^2\delta_\gamma^3$$
$$+7\,(329P+58)\,\gamma^3\delta_\gamma^2 + 6\,(181P+31)\,\gamma^4\delta_\gamma + 36\,(6P+1)\,\gamma^5,$$

$$\mathcal{G}_3 = 3\,(8P+3)\,\delta_\gamma^2 + (144P+35)\,\gamma\delta_\gamma + 8\,(6P+1)\,\gamma^2,$$

$$\mathcal{G}_4 = 19\,(17P+3)\,\delta_\gamma^4 + 3\,(599P+105)\,\gamma\delta_\gamma^3 + (2866P+481)\,\gamma^2\delta_\gamma^2$$
$$+ (1740P+277)\,\gamma^3\delta_\gamma + 66\,(6P+1)\,\gamma^4.$$

(B2)

3.   Functions for Eq. (57)

$$\mathcal{H}_{11} = k\,\hat{k}\,\bar{p}^2 + \hat{k}^2 p^2 + Pk\left(k - \delta_\gamma \alpha\right);$$

$$\mathcal{H}_{12} = P\alpha\left[\alpha\,\hat{\gamma}^2 + k\left(5\,\hat{\gamma} + 2\,\gamma\right)\right] - k\,\hat{k}\,\bar{p}^2 - \left(\hat{k}\,p\right)^2;$$

$$\mathcal{H}_{13} = (2P - 1)\,k^2 + \alpha\,k\left[P\left(5\,\hat{\gamma} + 2\,\gamma\right) - \hat{\gamma}\left(2\bar{p}^2 - p^2\right)\right] + \bar{p}\,\hat{\gamma}^2\,\alpha^2\delta_p;$$

$$\mathcal{H}_{14} = \hat{k}^2\left(\bar{p}^2 + p^2\right) - 2\,P\,k\,\alpha\,\hat{\gamma};$$

$$\mathcal{H}_{15} = k^2\delta_p^2 + k\,\alpha\left[(1 - 16\,P)\,\delta_\gamma + (1 - 12\,P)\,\gamma\right] - 4\,P\,\gamma^2\,\alpha^2;$$

$$\mathcal{H}_{16} = \hat{k}^2\bar{p}^2 + k\,\hat{k}\,p^2 + P\,k\left(k - \delta_\gamma\,\alpha\right);$$

$$\mathcal{H}_{21} = 4\left(\hat{\gamma}\,p + \gamma\,\bar{p}\right)k^3 + pk^2\alpha\left[\left(4p^2 + 5\right)\delta_\gamma^2 + (8p + 1)\,\gamma\delta_\gamma + 10\gamma^2\right]$$
$$+k\,\hat{\gamma}\,\alpha^2\left[p\left(5p^2 + 1\right)\delta_\gamma^2 + 8p^2\gamma^2 + 2\,m\,\alpha\,\gamma\left(6p^2 - 4P\right)\right] + p^3\alpha^3\gamma^3\left(\hat{\gamma} + \gamma\right);$$

$$\mathcal{H}_{31} = 4k^3\left(\hat{\gamma}p - \gamma\delta_p\right) + \left[p\left(9p^2 + 10P - 3\,\bar{p}^2\right)k^2\delta_\gamma^2\alpha + 2\left(4p^3 + 9pP + 8\,\bar{p}\,P + \bar{p}^3\right)\gamma\delta_\gamma^2\right.$$
$$+\gamma^2\left(10\,\bar{p}^2 - p^2 + 5P\right)\right] + k\,\alpha^2\,\hat{\gamma}\left[p\left(6p^2 + 2P - \bar{p}^2\right)\delta_\gamma^2 + \gamma\left(4p^3 + 8pP + 9\,\bar{p}\,P - 2\,\bar{p}^3\right)\delta_\gamma\right.$$
$$+2\gamma^2\left(5\bar{p}^3 - p^3 - pP + 4\bar{p}P\right)\right] + \alpha^3\,\delta_\gamma^2\left[\left(\gamma^2 + 2\,\gamma\,\hat{\gamma}\right)p^3 + 2\hat{\gamma}\,\gamma\,p\,P + 4\gamma^2\bar{p}^3\right];$$

$$\mathcal{H}_{22} = p^2\alpha^2\hat{\gamma}^3\left(\hat{\gamma} + \gamma\right) + k\,\alpha\,\hat{\gamma}\left[5p^2\delta_\gamma^2 + 4p\gamma^2 + 2\left(5p - 1\right)\gamma\delta_\gamma\right]$$
$$+k^2\left[4p^2\delta_\gamma^2 + 2\gamma^2 + (4p + 1)\,\gamma\delta_\gamma\right];$$

$$\mathcal{H}_{32} = k^2\left[\delta_p\gamma^2 - 4P\delta_\gamma\gamma + 4\left(1 + P\right)\delta_\gamma^2\right] + k\,\alpha\,\hat{\gamma}\left[p\left(2 + 3p\right)\delta_\gamma^2\right.$$
$$+\left(p^2 - 3\,\bar{p}^2\right)\gamma^2 + \left(2p^2 - 2P + 3\bar{p}^2\right)\gamma\,\delta_\gamma\right] + (\gamma\,\alpha)^2\left(\hat{\gamma}p - \gamma\right)\left(\hat{\gamma}\,p - 2\gamma\delta_p\right);$$

$$\mathcal{H}_{23} = \bar{p}^2 \alpha^2 \hat{\gamma}^3 \left(\hat{\gamma} + \gamma\right) + k \, \alpha \, \hat{\gamma} \left[4\bar{p}\gamma^2 + 2\left(4\bar{p} - p\right)\delta_\gamma \gamma + 5\bar{p}^2 \delta_\gamma^2\right]$$
$$+ k^2 \left[2\gamma^2 + \left(4\bar{p} + 1\right)\gamma \delta_\gamma + 4\left(\bar{p}\,\delta_\gamma\right)^2\right];$$

$$\mathcal{H}_{33} = k^2 \left[\left(1 + 4P\right)\gamma \delta_\gamma + 4\left(1 + p\right)\bar{p}\,\delta_\gamma^2 - \delta_p \gamma^2\right]$$
$$+ k \, \alpha \, \hat{\gamma} \left[\bar{p}\left(2 + 3p\right)\delta_\gamma^2 + \gamma^2 \left(\bar{p}^2 - 3p^2\right) + \gamma \delta_\gamma \left(3p^2 - 2P + 2\bar{p}^2\right)\right]$$
$$+ \left(\hat{\gamma}\,\alpha\right)^2 \left(\gamma \bar{p} - \gamma\right)\left(2\gamma \delta_p + \gamma \bar{p}\right)$$

$$\mathcal{H}_{24} = P\alpha^2 \hat{\gamma}\left(\hat{\gamma} + \gamma\right) + k \, \alpha \, \hat{\gamma} \left[\left(5P + 1\right)\delta_\gamma^2 + 5\gamma\,\delta_\gamma + 2\,\gamma^2\right] + 4k^3 m$$
$$+ k^2 \left[\left(4P + 1\right)\delta_\gamma^2 + 9\gamma\delta_\gamma + 2\gamma^2\right];$$

$$\mathcal{H}_{34} = 4k^3 \hat{\gamma} - k^2 \alpha \left(9\gamma^2 - 4P\gamma\delta_\gamma + 4P\delta_\gamma^2\right)$$
$$+ P \, k \, \alpha^2 \, \hat{\gamma} \left(2\delta_\gamma^2 + 7\delta_\gamma \gamma - 2\gamma^2\right) + p \, \alpha^2 \hat{\gamma}^3 \left(\hat{\gamma} - 4\gamma\right);$$

$$\mathcal{H}_{25} = 2P \, \alpha \, \hat{\gamma}^3 \left(\hat{\gamma} + \gamma\right) + k \, \hat{\gamma} \left(10 \, P \, \delta_\gamma^2 + 5\gamma \, \delta_\gamma + 2\gamma^2\right) + 2 \, k^2 m \left(\gamma + 4 \, P \, \delta_\gamma\right);$$

$$\mathcal{H}_{35} = \alpha \, \hat{\gamma}^3 \left[2\hat{\gamma}P + \gamma\left(1 - 8P\right)\right] + k \, \hat{\gamma} \left[6 \, P \, \delta_\gamma^2 - \left(1 - 14P\right)\gamma \, \delta_\gamma + \left(\delta_p^2 \, \gamma\right)\right] - 2 \, k^2 m \left(\gamma \, \delta_p^2 + 4 \, P \, \delta_\gamma\right);$$

$$\mathcal{H}_{26} = 4 \, k^3 \left(\hat{\gamma} \, \bar{p} + \gamma \, p\right) + \bar{p} \, \alpha \, k^2 \left[\left(4\bar{p}^2 + 1\right)\delta_\gamma^2 + 10 \, \gamma^2 + \left(8 \, \bar{p} + 1\right)\gamma \, \delta_\gamma\right]$$
$$+ k \, \hat{\gamma} \, \alpha^2 \left[\bar{p}\left(5 \, \bar{p}^2 + 1\right)\delta_\gamma^2 + 2\left(p^2 - 2P + 7\bar{p}^2\right)\gamma \, \delta_\gamma + 8\left(\bar{p} \, \gamma\right)^2\right] + \left(\bar{p} \, \alpha \, \hat{\gamma}\right)^3 \left(\hat{\gamma} + \hat{\gamma}\right);$$

$$\mathcal{H}_{36} = 4\left(\gamma \, \delta_p + \hat{\gamma} \, \bar{p}\right) k^3 + \left[\bar{p}\left(9 \, \bar{p}^2 - 3 \, p^2 + 10P\right) k^2 \, \alpha \, \delta_\gamma^2\right.$$
$$+ 2\left(p^3 + 8pP + 9 \, \bar{p}P + 4 \, \bar{p}^3\right)\gamma \, \delta_\gamma + \left(10 \, p^2 + 5P - \bar{p}^2\right)\gamma^2\right]$$
$$+ \left[\bar{p}\left(6 \, \bar{p}^2 - p^2 + 2 \, P\right) k \, \alpha^2 \, \hat{\gamma} \, \delta_\gamma^2 + \left(4 \, \bar{p}^3 - 2p^3 + 9pP + 8 \, \bar{p} \, P\right)\gamma \, \delta_\gamma\right.$$
$$\left. - 2\left(5p^3 + 4pP - \bar{p}P - \bar{p}^3\right)\gamma^2\right]$$
$$+ \hat{\gamma}^2 \alpha^3 \left[\delta_\gamma^2 \, \bar{p}^3 + 2 \, \bar{p} \, P \, \delta_\gamma \, \gamma + \gamma^2 \left(4p^3 - 2 \, \bar{p} \, P - \bar{p}^3\right)\right].$$

[1] K. Huang, *Statistical Mechanics* (Willey, New York, 1987); Y. Demirel, *Nonequilibrium thermodynamics: transport and rate processes in physical and Biological systems* (Amsterdam: Elsevier); R. Klages, W. Just, and C. Jarzynski, editors, *Nonequilibrium Statistical Physics of Small Systems: Fluctuation Relations and Beyond* (Wiley-VCH Verlag, Weinheim, 2013).

[2] T. S Druzhinina, S. Hoeppener, and U. S. Schubert, *Nano Lett.* **10**, 4009 (2010).

[3] A. A. Balandin, *Nat. Materials* **10**, 569 (2011).

[4] S. Schnell, T. J. H. Vlugt, J.-M. Simon, D. Bedeaux, and S. Kjelstrup, *Chem. Phys. Lett.* **504** 199 (2011).

[5] K. Fujita, M. Iwaki, A. H. Iwane, L. Marcucci, and T. Yanagida, *Nat. Commun.* **3**, 956 (2012).

[6] A. Levy and R. Kosloff, *Phys. Rev. Lett.* **108**, 070604 (2012).

[7] M. Osiak, W. Khunsin, E. Armstrong, T. Kennedy, C. M. Sotomayor Torres, K. M. Ryan, and C. ODwyer, *Nanotechnology* **24**, 065401 (2013).

[8] T. Czernik, J. Kula, J. Łuczka, and P. Hänggi, *Phys. Rev.* E **55**, 4057 (1997).

[9] A. Baule and E. G. D. Cohen, *Phys. Rev.* E **79**, 030103 (2009).

[10] W. T. Coeffly, D. A. Garanin, and D. J. McCarthy, *Adv. Chem. Phys.* **117** 483 (2001).

[11] D. Applebaum, *Lévy Processes and Stochastic Calculus* (Cambridge University Press, Cambridge, 2004).

[12] W. A. M. Morgado and S. M. Duarte Queirós, *Phys. Rev.* E **86**, 041108 (2012).

[13] W. A. M. Morgado and S. M. Duarte Queirós, and D. O. Soares-Pinto, *J. Stat. Mech.* (2011) P06010; 1997; W. A. M. Morgado and S. M. Duarte Queirós (submitted to Phys. Rev. E, 2015).

[14] K. Kanazawa, T. Sagawa, and H. Hayakawa, *Phys. Rev.* E **87**, 052124 (2013).

[15] K. Kanazawa, T. G. Sano, T. Sagawa, and H. Hayakawa, *Phys. Rev. Lett.* **114** 090601 (2015); K. Kanazawa, T. G. Sano, T. Sagawa, and H. Hayakawa, *J. Stat. Phys.* **160** 1294 (2015).

[16] G. H. Weiss, *J. Stat. Phys.* **15**, 157 (1976).

[17] F. Julicher, A. Ajdari, and J. Prost, *Rev. Mod. Phys.* **69** 1269, (1997).

[18] C. R. Doering and J. C. Gadova, *Phys. Rev. Lett.* **69** 2318, (1992).

[19] L. Novotny, R. X. Bian and X. S. Xie, *Phys. Rev. Lett.* **79**, 645 (1997).

[20] B. van der Pol and H. Bermmer, *Operational Calculus Based on the Two-Sided Laplace Integral* (Cambridge University Press, Cambridge, 1950). E. Gluskin, *Eur J Phys* **24** 591, (2003).

[21] M. J. I. Müller, S. Klumpp, and R. Lipowsky, *Biophys. J.* **98**, 2610 (2010).

[22] A. Gitterman, *Physica* A **221**, 330 (1995).

[23] A. B. Kolomeisky and M. E. Fisher, *Annu. Rev. Phys. Chem.* **58**, 675 (2007).

[24] G. Pfister and H. Scher, *Adv. Phys.* **27**, 747 (1978).

[25] J. Giddings and H. Eyring, *J. Phys. Chem.* **59**, 416 (1955).

[26] C. R. de Oliveira, C. M. Arizmendi, and J. Sanchez, *Physica* A **330**, 400 (2003).

[27] Y. Jung, E. Barkai, and R. J. Silbey, Chem. Phys. **284**, 181 (2002).

[28] R. G. Neuhauser, K. T. Shimizu, W. K. Woo, S. A. Empedocles, and M. G. Bawendi, *Phys. Rev. Lett.* **85**, 3301 (2000).

[29] J. Łuczka, T. Czernik, and P. Hänggi, *Phys. Rev.* E **56**, 3968 (1997).

[30] M. O. Cáceres and A. A. Budini, *J. Phys.* A **30**, 8427 (1997); M. O. Cáceres, *Phys. Rev.* E **67**, 016102 (2003).

[31] P. Allegrini, P. Grigolini and B. J. West, *Phys. Rev.* E **54**, 4760 (1996); P. Allegrini, P. Grigolini, L. Palatella and B. J. West, *Phys. Rev.* E **70**, 046118 (2004).

[32] N. G. van Kampen *Stochastic Processes in Physics and Chemestry* (Elsevier, Amsterdam, 2007).

[33] J. Marcinkiewicz, *Math. Z.* **44**, 612 (1938).

[34] H. Mori, *Prog. Theo. Phys.* **33**, 423 (1965); R. Kubo, editor, *1965 Tokyo Summer Lectures in Theoretical Physics* (Benjamin, New York, 1966).

[35] F. D. Nobre, E. M. F. Curado, A. M. C. Souza and R. F. S. Andrade, *Phys. Rev.* E **91**, 022135 (2015).

[36] Y. Yura, H. Takayasu, D. Sornette and M. Takayasu, Phys. Rev. Lett. **112**, 098703 (2014).